International Journal of Applied Power Engineering (IJAPE)
Vol. 15, No. 1, March 2026, pp. 393~402
ISSN: 2252-8792, DOI: 10.11591/ijape.v15.i1.pp393-402

Blade number and angle effect the archimedes spiral wind turbine performance

Rosadila Febritasari, Muhammad Ibnul Abidin
Department of Mechanical Engineering, Faculty of Industrial Technology, Malang National Institute of Technology, Malang, Indonesia

Article Info

Article history:

Received May 16, 2024
Revised Dec 4, 2025
Accepted Jan 9, 2026

Keywords:

Archimedes wind turbine
Coefficient of moment
Computational fluid dynamic
Spiral blade
Wind energy

ABSTRACT

The efficiency and performance of Archimedes spiral wind turbine (ASWT) are affected by the design and number of turbine blades which can convert the kinetic energy of the wind into mechanical energy to turn a generator that can produce electricity as much as possible in low wind speed. This study aims to obtain the optimal ASWT design in low wind speed in terms of aerodynamic performance. The method is conducted by numerically computational fluid dynamics (CFD) simulation on the fixed-opening angle and the blades number variations. The results show that the smallest C_D value is -2.18 at the 65° of opening angle, the largest C_L value at the 45° of opening angle is 0.37, and the largest C_M value is 0.61 at the 65° of opening angle and 4 blades. Therefore, it can be concluded that the Archimedes wind turbine with 4 blades and 65° pitch is the optimal.

Corresponding Author:

Rosadila Febritasari
Department of Mechanical Engineering, Malang National Institute of Technology
Karanglo Street, Malang, East Java, Indonesia
Email: rosadila@lecturer.itn.ac.id

1. INTRODUCTION

Energy has become a world problem in a few years, because the energy sources that have been used so far, such as petroleum, natural gas, and coal, are non-renewable energy sources and are increasingly scarce [1], [2]. This problem encourages many technicians and scientists to use new and renewable energy sources. This energy does not depend on quantity because it comes from a sustainable nature. Wind energy is one of the renewable energies that can be used as an energy source with the help of wind turbines or windmills. Mechanical energy gathered from the wind, such as torque and speed can be used directly or converted into electrical energy [3]. Many kinds of wind turbines have been developed with different axis configurations, different airfoil-profile blades, different shapes and sizes, and many others that can achieve different aerodynamics performance and enhance the energy efficiency [4], [5]. Recently, the researchers investigated several wind turbines that can achieve high performance in power generated at low wind speed [6].

Various scientific research about wind turbine efficiency and optimization have been worked. An analysis of lift force, drag force, and pressure coefficient for the NACA S814 blade profile used in horizontal axis wind turbines (HAWT) was presented in [7]. The modification of the NACA 0012 airfoil at various angles of attack and its evaluation at Reynolds numbers of 1,000 and 5,000 were reported in [8], showing that both lift and drag forces increase as the Reynolds number rises. The vertical axis wind turbine (VAWT) was analyzed using computational fluid dynamics (CFD) in [9] to obtain an optimized turbine design. From those researches, the HAWT and VAWT are kind of large size turbines that need heavy machinery to install. The installation and maintenance of those are a difficult process because of the tall tower and heavy turbines. So, those are not suitable for urban use [10].

One of the wind turbines that can be installed on homes or cities is the archimedes spiral wind turbine (ASWT) [11], which generates less noise than other turbines due to its very low rotational speed in low-speed wind conditions. The profile of the ASWT blade is spiral like a natural creature, Thatcheria mirabilis, which causes the ASWT can automatically align to the direction of the wind without any yaw apparatus [12], which means the ASWT has the ability to adjust for changes in wind direction. A biomimetic design study of ASWT blades incorporating spanwise grooves inspired by the ventral pleats of rorqual whales demonstrated an 8.3% increase in power coefficient at 10 m/s, while surface bumps led to reduced performance [13]. The ASWT is classified in horizontal axis and designed on Archimedes spiral principle. It can produce energy from the wind by redirecting its flow 90 degrees relative to the original direction. Related researches about ASWT were demonstrated that this turbine operates as a horizontal-axis drag-type rotor obtained a maximum power coefficient of 0.293 at a tip-speed ratio of 2.19, and additional generator–controller testing provided the electrical efficiency needed to predict the full power curve [14]. Further development of a three-bladed ASWT with opening angles of 35°, 45°, and 65° was presented in [15], which analyzed the lift (C_L) and drag (C_D) coefficients and showed that C_L increased with larger opening angles at a wind speed of 5.5 m/s. An investigation focusing on blade opening angle design was carried out in [16], where numerical and experimental tests demonstrated that the variable-angle configuration produced 14.7% higher output than the fixed-angle design. The influence of blade angle on the aerodynamic performance of ASWT was examined in [17], showing that increasing the blade angle reduced the maximum rotational speed and output power, suggesting that Archimedes aerofoil wind turbines perform optimally under moderate to light wind conditions. Wake flow characteristics of ASWT were analyzed in [18], showing that interactions between downstream wake flow and tip-vortex-induced velocity were strongly influenced by wind speed and blade rotational speed. A comparative numerical study using ANSYS fluent in [19] examined spiral wind turbines with three different blade profiles, concluding that the Archimedean spiral with a 60° opening angle provided the best aerodynamic performance.

The new finding with contrast to the previous works is the number of Archimedes spiral blade effects. The blade number should be taken care of carefully in designing the wind turbine especially the ASWT because it can affect the manufacturing process, the fabricated cost and the aerodynamics which mean the efficient blade number is able to increase the wind energy [20]. The main theme of this study is the blade design of ASWT. The specific goal of this study is to obtain the optimum design of ASWT by numerical investigation in various numbers of blades in 2, 3, and 4 blades and modified each blade with the opening angle variations in 45°, 55°, and 65°. This study is developed following two steps such as designing the ASWT with both parameters using CAD Software, then simulating the ASWT designs using CFD Software. The simulation results are the value of the drag coefficient (C_D), lift coefficient (C_L) and moment coefficient (C_M) for various variations in the number of blades and the blade angles. The values of C_D, C_L, and C_M are relevant to aerodynamics performance in wind turbines which indicated the efficiency of the fluid flow through the turbine.

2. METHOD

This study is conducted by numerical simulation of ASWT by following the methods as follows: First, the literature study is conducted by searching the reference of ASWT and finding out the gap analysis of related research. The ASWT are characterized by its unique spiral blade design, which differentiates them from conventional horizontal and vertical axis wind turbines. The previous studies had analyzed the performance of ASWT that generally evaluated the opening angle in three blades to enhance the energy capture in low wind speed. The research gap is the analysis of blade number variation and the opening angle to capture the complex airflow interactions around spiral blades. Beside that, the efficiency model is investigated especially for small-scale or residential applications. Second, the 3D modeling of ASWT's blade is designed using CAD Software. This blade turbine is designed in laboratory-scaled size. The blade is only constructed because this study only investigated the fluid flow through the blade. There are 9 different blade models including the fixed-opening angle (θ=45°, 55°, 65°) and the number of blades (n = 2, 3, 4). Third, the 3D model is imported into the simulation software to analyze the fluid dynamics occurring in these turbines [21]. This simulation is based on CFD that detailed airflow patterns around the blades with a turbulence model. The simulation approached the environmental conditions to assess turbine performance, such as the wind speed is at 7 m/s, the wind direction is from the inlet section of the boundary wall, the temperature and pressure are modeled with standard atmospheric conditions. Fourth, the preprocessing stage in simulation is set, such as generating the mesh, setting the boundary conditions and parameters, determining the fluid flow model and material properties, determining the scheme and discretization, then determining the governing equation. The simulation stage is conducted by running the simulation. The details of the preprocessing stage are explained in the next section. The turbine will be analyzed by wind speed, pressure, and airflow.

The simulation will reach the convergence iteration. The results provide qualitative and quantitative data. The qualitative data shows the illustration of airflow across the ASWT to interpret performance trends and identify potential areas for improvement, and the quantitative data provides the coefficient of drag (C_D), coefficient of lift (C_L), and coefficient of moments (C_M) to assess variability and significance of results.

2.1. ASWT design

The ASWT is a sort of HAWT. This turbine has some blades with spiral shape that adopt Archimedes configuration [22]. This unique blade shape can use drag force to capture wind energy instead of using lift force produced by air pushed down by an aerodynamic shape (airfoil) like a conventional HAWT does. The focus of this study is the design of ASWT that can be seen in Figure 1. The parameter used in ASWT such as r indicates the turbine radius means the radial distance between the blade tip at the exit and the axis of rotation, θ indicates the opening angle blade means the angle between the axis rotation and the blade tip at the outlet, L indicates the length of turbine means the distance between the blade tip at the beginning and the end, and n indicates the number of blades.

In the presented study, the ASWT performance is focused on the fixed-opening angle and the number of blades. Table 1 presents different ASWT design with variation in the fixed-opening angle ($\theta = 45°, 55°, 65°$) and the number of blades ($n = 2, 3, 4$). Those designs will cause aerodynamic interaction between spiral blade design and wind flow. The diameter of the ASWT is 150 mm and the motor streamwise length is 305 mm along the rotational axis. The model only focused on blade turbines, the bolt and nut geometry had been simplified, and also the generators and other components had been removed. The blade material is ignored because the blade material is not effected by the CFD simulation.

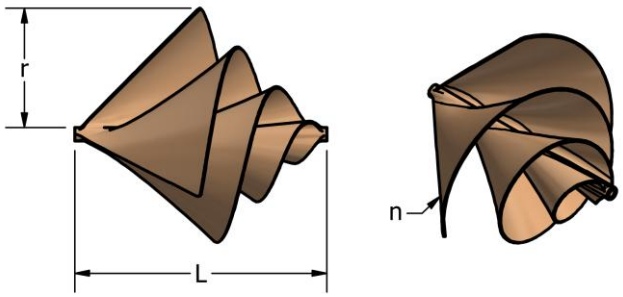

Figure 1. Definition of the parameters used in the ASWT design form side and isometric view

Table 1. The different design of ASWT based on the opening angle and the number of blades

Blade number	$\theta = 45°$	$\theta = 55°$	$\theta = 65°$
$n = 2$	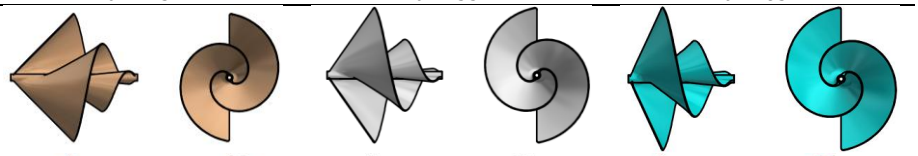		
$n = 3$			
$n = 4$	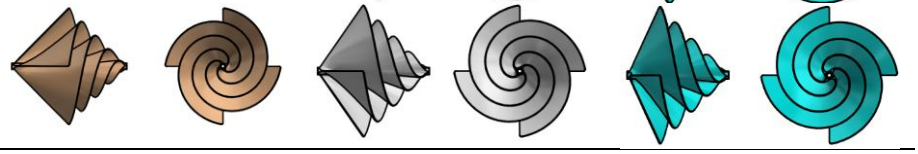		

2.2. Numerical methodology

This study is conducted numerically using CFD which utilized the Software simulation as the instrumental. It is aimed to obtain the ASWT performance, such as the coefficient of drag (C_D), Coefficient of Lift (C_L), and coefficient of moments (C_M). The simulation procedure can be seen in Figure 2, which shows that three stages of procedures should be followed step by step from pre-processing stage until post-processing stage.

Figure 2 explains the simulation procedure that is started from the pre-processing stage until the post-processing stage. The mesh is generated for the simulation. The mesh type used is a tetrahedron with 10 mm of mesh size. The quality of mesh generation is checked and the result can be seen in Table 2.

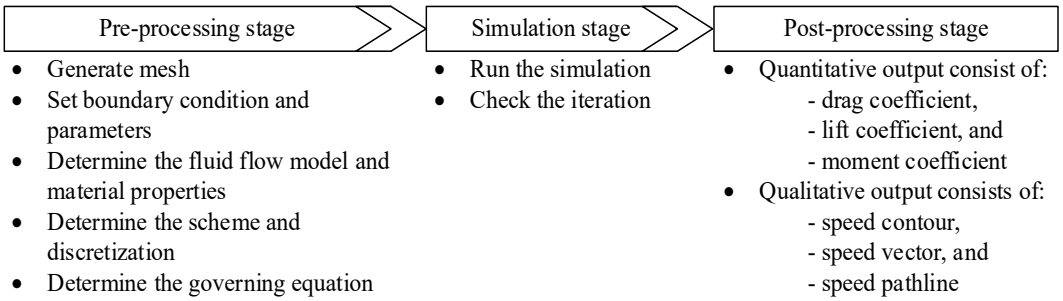

Figure 2. The simulation procedure

Table 2. The elements and nodes of mesh contained in ASWT models

Fixed-opening angle:	45°		55°		65°	
Blade number	Nodes	Elements	Nodes	Elements	Nodes	Elements
$n = 2$	122,193	644,432	115,055	607,738	108,513	573,694
$n = 3$	141,655	746,281	132,271	696,364	128,364	675,892
$n = 4$	141,103	735,686	133,882	700,491	153,370	799,341

The boundary condition is set in cylindric shape, then the ASWT rotor's center is placed at 2D distance from the inlet and a 8D distance from the outflow, as shown in Figure 3. The surface sections are set as inlet velocity, wall, and outlet pressure. The fluid material is air or wind. This study configures the fluid flow model as *SST* $k - \omega$ model and illustrates the airflow across the ASWT, which adopted from [23], shown in Figure 4. The simulation will show the force generated by the rotor surface. In the pre-processing stage, the model that had been generated in CAD Software was imported into simulation software.

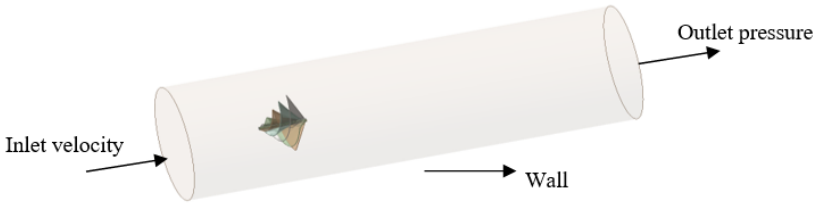

Figure 3. Boundary condition

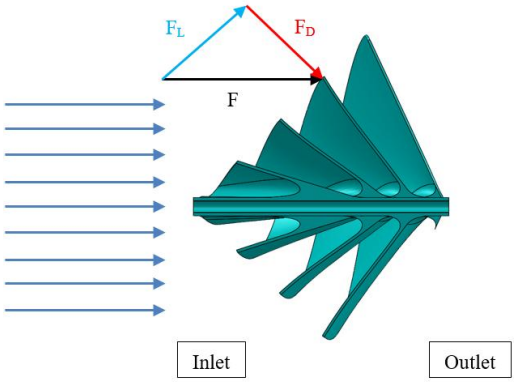

Figure 4. The illustration of aerodynamic force analysis on the ASWT rotor

This study was solved using the governing equations such as the time-averaged continuity as shown in (1) and the momentum equation for steady flow as (2) [10], [24]:

$$\frac{\partial U_i}{\partial x_i} = 0 \tag{1}$$

Where the time-averaged continuity equation as in (1) uses U_i to indicate the average velocity vector in three dimensions.

$$\rho\bar{u}_j\left(\frac{\partial\bar{u}_i}{\partial x_j}\right) = \frac{\partial\bar{p}}{\partial x_i} + \mu\frac{\partial}{\partial x_j}\left[\frac{\partial\bar{u}_i}{\partial x_j} + \frac{\partial\bar{u}_j}{\partial x_i}\right] - \frac{\partial}{\partial x_j}\left(\rho\overline{u'_\iota u'_\jmath}\right) \tag{2}$$

The total convective change as in (2) in mean momentum consists of the three terms on the lefthand side. The first term is pressure field that is written in $\bar{p}$. The second term is viscous term that is written in $\frac{\partial}{\partial x_j}\left[\frac{\partial\bar{u}_i}{\partial x_j} + \frac{\partial\bar{u}_j}{\partial x_i}\right]$. This viscous term can create stress. The third term is the Reynolds stress that is interpreted by $\left(\rho\overline{u'_\iota u'_\jmath}\right)$ in the mean turbulent velocity fluctuations. The notation of the equations such as ρ shows density (kg/m^3) which is 1.225 kg/m^3, μ means the fluid viscosity (N.s/m^2), $\overline{u'_\iota}$ and $\overline{u'_\jmath}$ indicate the velocity fluctuation components (m/s). The subscripts i and j present the free indices. The i and j can be written in $1, 2, 3$ of number to represent the x, y and z directions respectively. The model used in this study is *SST* $k-\omega$ model which is calculated in two additional transport equations, such as k is the kinetic turbulent energy and ω is the specific turbulent dissipation rate. The SST k-ω turbulence model demonstrated superior performance by providing the most accurate and consistent predictions of aerodynamic torque, pressure distribution, and flap-wise bending loads across various wind speeds compared to the other models tested [25]. Those equation is written as in (3) and (4).

$$\frac{\partial k}{\partial t} + u_j\frac{\partial k}{\partial x_j} = P_k - \beta^* k\omega + \frac{\partial}{\partial x_j}\left[\left(v + \sigma_{k_1}v_T\right)\left(\frac{\partial k}{\partial x_j}\right)\right] \tag{3}$$

$$\frac{D_\omega}{D_t} = \frac{\gamma_1}{v_T}\tau_{ij}\left(\frac{\partial u_i}{\partial x_j}\right) - \beta_1\omega^2 + \frac{\partial}{\partial x_j}\left[\left(v + \sigma_{k_1}v_T\right)\left(\frac{\partial\omega}{\partial x_j}\right)\right] \tag{4}$$

The SST $k-\omega$ model as in (3) and (4) consist of constants such as $\sigma_{k_1} = 0.85, \sigma_1\omega = 0.5$, $\beta_1 = 0.075, \beta^* = 0.09, k = 0.41$, and $\gamma_1 = \frac{\beta_1}{\beta^*} - \frac{\sigma_1\omega k^2}{\sqrt{\beta^*}}$. The term v_T that indicates the turbulent kinematic eddy viscosity can be represented in (5).

$$v_T = \frac{\mu_T}{\rho} = \frac{k}{\omega} = \frac{a_{1k}}{\max(a_1\omega, \Omega_{strain-rate})} \tag{5}$$

Where $\Omega_{strain-rate}$ as written in (5) is the shear strain rate, a_1 is a proportionality constant that can be obtained from $\tau = a_1\rho k$ and k is the turbulent kinetic energy.

The scheme was set for the second-order upwind and central difference, then the discritization adjusted in the kinetic turbulent energy k and the specific turbulent dissipation rate ω. Then, the pressure velocity coupling is carried out through the semi-implicit method for pressure-linked equations. The solver was pressure based. The boundary conditions at inlet and outlet boundaries were adjusted in 1% of turbulence intensity and 1 of turbulence viscosity ratio. The domain wall and the solid boundaries were set with no-slip adiabatic conditions.

In the simulation stage, this study measures the coefficient of drag (C_D), coefficient of lift (C_L), and coefficient of moments (C_M). The simulation results in different values for each different ASWT design. The lift coefficient that used to represent the lift force (F_L) that is generated by lifting the body to the fluid density, the fluid velocity and an associated reference area. In a turbine, the lift value increases by increasing the angle of attack and turbulence on the active surface. The drag coefficient that used to represent the drag force (F_D) on an ASWT that moves through a fluid which means the ASWT's aerodynamic or hydrodynamic. In a turbine, a lower drag coefficient indicates the turbine will have less aerodynamic or hydrodynamic drag. C_M is a constant number of the moment of inertia possessed by a rigid object whose value is determined by the shape and axis of rotation of the object [26]. Those are important parameters that affect the ASWT performance. To obtain those coefficient values, the convergence value should be monitored within 1e-3 of residue with the time step size is at 1e-3 and the number of time steps is at 5e+5.

3. RESULTS AND DISCUSSION

This paper investigates the changes of different parameters in terms of the coefficient of drag (C_D), coefficient of lift (C_L), and coefficient of moments (C_M). These investigations are conducted using CFD simulation. CFD performs the simulation and solves the flow governing equations around the turbine blade for each nine different ASWT's designs in 7 m/s of wind speed. Then, the results of the variations of the fixed-opening angle $(\theta = 45°, 55°, and\ 65°)$ and the number of blades $(n = 2, 3, and\ 4)$ are discussed. A comparison of the fixed-opening angle in terms of C_D and C_L is presented in Figure 5. And a comparison of the 9 different ASWT's designs in terms of C_M is shown in Figure 6.

Figure 6 shows that the smallest C_D value is for the spiral blade with an angle of 65° and the highest C_L value is for the spiral blade with an angle of 45°. In an ASWT with a small fixed-opening angle, undisturbed free flow can pass through the blades more easily than with a large one. Therefore, an ASWT with a large fixed-opening angle has a stronger air blocking effect than a rotor with a small one, and a stronger blocking effect forces more fluid to flow through the spiral blade region of the turbine. A positive C_D value means drag, and a negative C_D value means acceleration. It can be concluded that the spiral blade with an inclination of 65° has the best acceleration because the C_D value is the smallest.

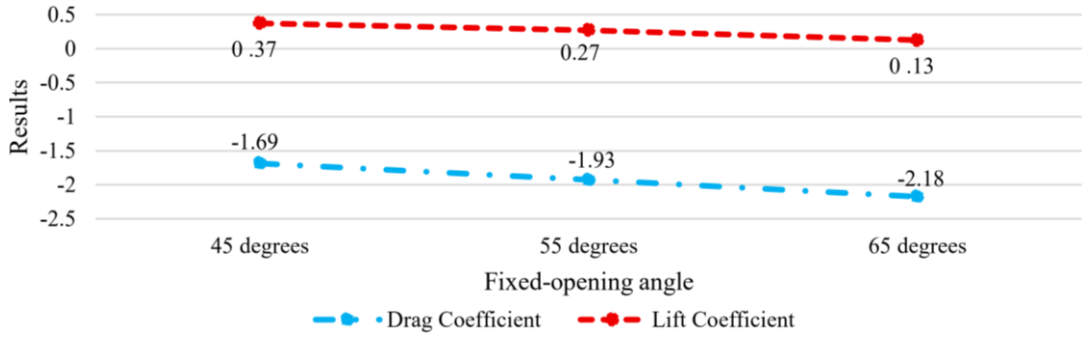

Figure 5. A comparison of the fixed-opening angle in terms of C_D and C_L

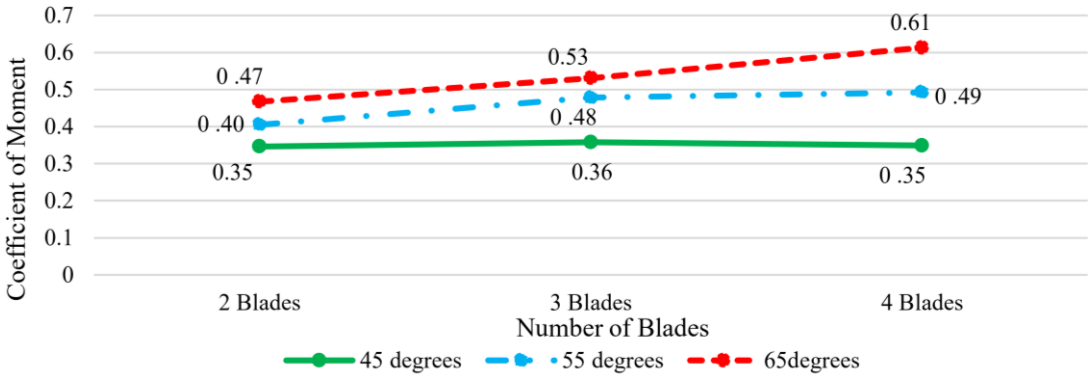

Figure 6. A comparison of the 9 different ASWT's designs in terms of C_M

The magnitude of the C_M value tends to increase as the number of blades and blade opening angle increase. A small coefficient of moment (C_M) value means that the rotary torque produced by the turbine is small, while a large coefficient of moment (C_M) value means that the rotary torque produced by the turbine is large, so the turbine has good performance. Figure 6 shows the smallest C_M value when varying 2 spiral blades with 45° of fixed-opening angle and the largest C_M value when varying 4 spiral blades with 65° of fixed-opening angle.

To compare the speed pathline around the ASWT surface obtained from the CFD simulations. Figures 7, 8, and 9 show the results at a constant wind speed of 7 m/s. These comparisons have been made using the pathline view in the CFD post-processing.

Figures 7, 8, and 9 show the illustration of airflow across the ASWT in terms of velocity pathline. The solution bar represents the color line in velocity magnitude. The red color indicates an increase in airflow velocity while the dark blue color shows a decrease in airflow velocity. The velocity magnitude can be seen in Table 3. The increase in airflow speed is because the air is captured by the turbine spiral blades so that it gathers in the center of the rotor with a subsequent increase in speed, which is shown by the red pathline speed. In addition, the highest speed region appears near the tip of the turbine rotor, while the lowest speed region appears behind the hub, resulting in turbulence in this area and reverse flow shown in the vector direction back to the inlet. This is caused by the effect of forming the direction of air flow after passing through the spiral turbine blade periodically. The same thing also happened in the research conducted by [12], namely the appearance of turbulent flow in the area behind the blade.

Table 3. The velocity magnitude

The fixed-opening angle		$\theta = 45°$	$\theta = 55°$	$\theta = 65°$
The number of blades	$n = 2$	20.9	20.2	21.7
	$n = 3$	19	23.1	25.1
	$n = 4$	19.4	23.4	27

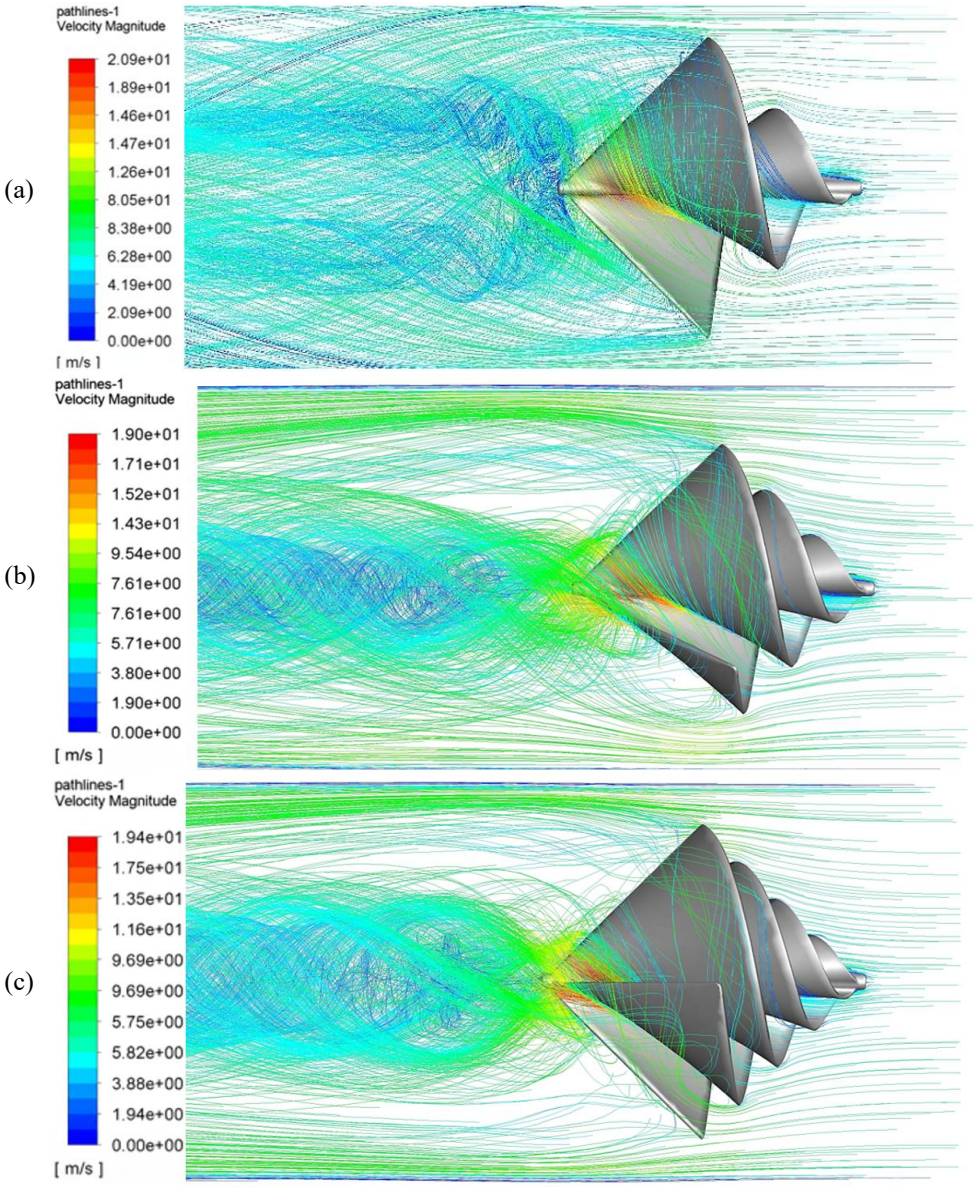

Figure 7. The comparison of the speed pathline around the ASWT with the 45° of fixed-opening angle: (a) 2 blades, (b) 3 blades, and (c) 4 blades

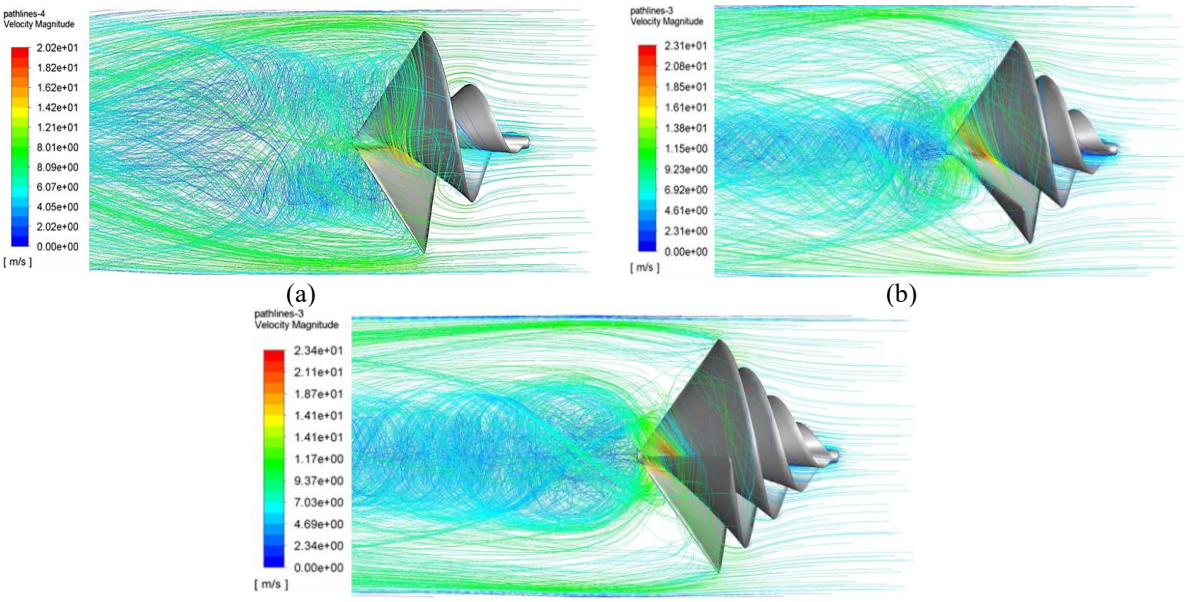

Figure 8. The comparison of the speed pathline around the ASWT with the 55° of fixed-opening angle: (a) 2 blades, (b) 3 blades, and (c) 4 blades

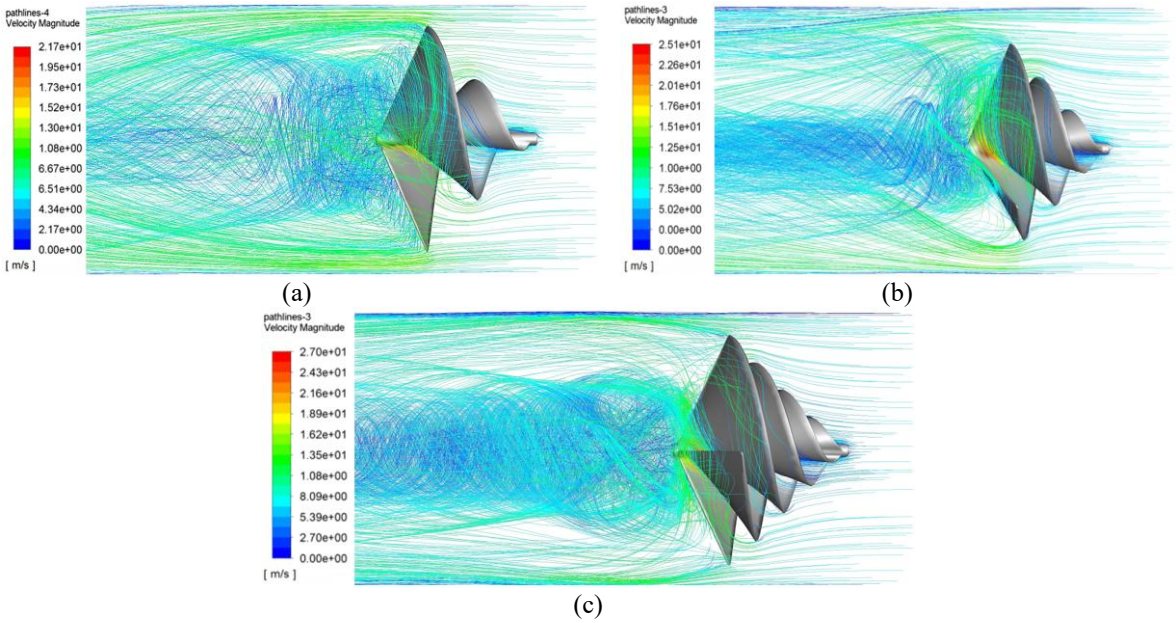

Figure 9. The comparison of the speed pathline around the ASWT with the 65° of fixed-opening angle: (a) 2 blades, (b) 3 blades, and (c) 4 blades

4. CONCLUSION

The variation of the fixed-opening angle is ASWT's blade affects the value of the C_D and C_L, such as fixed-opening angle is small means the C_D and C_L values increase, it can be seen that the 45° of fixed-opening angle has the largest C_D and C_L values, namely C_D = -1.69 and C_L = 0.37. The C_D and C_L decrease in the $\theta = 65°$ of fixed-opening angle with a value of C_D = -2.18 and C_L = 0.13. The magnitude of the coefficient of moment (C_M) is different in each turbine variation. The C_M in ASWT with 45° of fixed-opening angle has a 2.4% decline when it adds the number of blades in 4 blades. The enhancement occurs in ASWT with 65° of fixed-opening angle when the number of blades add, namely 23.51%, which is the highest C_M is in ASWT with 65° of fixed-opening angle and 4 blades.

ACKNOWLEDGMENTS

We must thank and appreciate the head of the Computer Laboratory in Mechanical Engineering Department, Faculty of Industrial Technology, Malang National Institute of Technology, who were providing the facilities to support this study.

FUNDING INFORMATION

Authors state no funding involved.

AUTHOR CONTRIBUTIONS STATEMENT

This journal uses the Contributor Roles Taxonomy (CRediT) to recognize individual author contributions, reduce authorship disputes, and facilitate collaboration.

Name of Author	C	M	So	Va	Fo	I	R	D	O	E	Vi	Su	P	Fu
Rosadila Febritasari	✓	✓		✓	✓	✓		✓	✓	✓		✓		
Muhammad Ibnul Abidin	✓	✓	✓	✓	✓	✓		✓	✓	✓	✓			

C : **C**onceptualization
M : **M**ethodology
So : **So**ftware
Va : **Va**lidation
Fo : **Fo**rmal analysis
I : **I**nvestigation
R : **R**esources
D : **D**ata Curation
O : Writing - **O**riginal Draft
E : Writing - Review & **E**diting
Vi : **Vi**sualization
Su : **Su**pervision
P : **P**roject administration
Fu : **Fu**nding acquisition

CONFLICT OF INTEREST STATEMENT

Authors state no conflict of interest.

DATA AVAILABILITY

The data that support the findings of this study are available from the corresponding author upon reasonable request.

REFERENCES

[1] B. M. Opeyemi, "Path to sustainable energy consumption: the possibility of substituting renewable energy for non-renewable energy," *Energy*, vol. 228, p. 120519, Aug. 2021, doi: 10.1016/j.energy.2021.120519.
[2] A. Shasavari, A. Karimi, M. Akbari, and M. A. Noughani, "Environmental impacts and social cost of non-renewable and renewable energy sources: a comprehensive review," *Journal of Renewable Energy and Environment*, vol. 11, no. 1, pp. 12–27, 2023.
[3] A. Chaudhuri, R. Datta, M. P. Kumar, J. P. Davim, and S. Pramanik, "Energy conversion strategies for wind energy system: electrical, mechanical and material aspects," *Materials*, vol. 15, no. 3, p. 1232, Feb. 2022, doi: 10.3390/ma15031232.
[4] K. Calautit and C. Johnstone, "State-of-the-art review of micro to small-scale wind energy harvesting technologies for building integration," *Energy Conversion and Management: X*, vol. 20, p. 100457, Oct. 2023, doi: 10.1016/j.ecmx.2023.100457.
[5] L. Bilir, M. İmir, Y. Devrim, and A. Albostan, "An investigation on wind energy potential and small-scale wind turbine performance at İncek region – Ankara, Turkey," *Energy Conversion and Management*, vol. 103, pp. 910–923, Oct. 2015, doi: 10.1016/j.enconman.2015.07.017.
[6] E. Simley, P. Fleming, N. Girard, L. Alloin, E. Godefroy, and T. Duc, "Results from a wake-steering experiment at a commercial wind plant: investigating the wind speed dependence of wake-steering performance," *Wind Energy Science*, vol. 6, no. 6, pp. 1427–1453, Nov. 2021, doi: 10.5194/wes-6-1427-2021.
[7] S. Aziz *et al.*, "Computational fluid dynamics and experimental analysis of a wind turbine blade's frontal section with and without arrays of dimpled structures," *Energies*, vol. 15, no. 19, 2022, doi: 10.3390/en15197108.
[8] B. S. Patil and H. R. Thakare, "Computational fluid dynamics analysis of wind turbine blade at various angles of attack and different Reynolds numbers," *Procedia Engineering*, vol. 127, pp. 1363–1369, 2015, doi: 10.1016/j.proeng.2015.11.495.
[9] A. A. Afif, P. Wulandari, and A. Syahriar, "CFD analysis of vertical axis wind turbine using ANSYS fluent," *Journal of Physics: Conference Series*, vol. 1517, no. 1, p. 012062, Apr. 2020, doi: 10.1088/1742-6596/1517/1/012062.
[10] M. A. Al-Rawajfeh and M. R. Gomaa, "Comparison between horizontal and vertical axis wind turbine," *International Journal of Applied Power Engineering (IJAPE)*, vol. 12, no. 1, p. 13, Mar. 2023, doi: 10.11591/ijape.v12.i1.pp13-23.
[11] A. G. Refaie, H. S. A. Hameed, M. A. A. Nawar, Y. A. Attai, and M. H. Mohamed, "Comparative investigation of the aerodynamic performance for several shrouded Archimedes spiral wind turbines," *Energy*, vol. 239, p. 122295, Jan. 2022, doi: 10.1016/j.energy.2021.122295.
[12] K. Song, H. Huan, and Y. Kang, "Aerodynamic performance and wake characteristics analysis of Archimedes spiral wind turbine rotors with different blade angle," *Energies*, vol. 16, no. 1, p. 385, 2023, doi: 10.3390/en16010385.
[13] A. E. Faisal, C. W. Lim, B. A. J. Al-Quraishi, J. Milano, T. C. Hong, and C. P. Chen, "Aerodynamic performance enhancement of Archimedes spiral wind turbine blades through surface modifications: a numerical and experimental study," *Scientific Reports*, vol. 15, no. 1, p. 41112, Nov. 2025, doi: 10.1038/s41598-025-24908-6.

[14] H. Jang, D. Kim, Y. Hwang, I. Paek, S. Kim, and J. Baek, "Analysis of Archimedes spiral wind turbine performance by simulation and field test," *Energies*, vol. 12, no. 24, p. 4624, Dec. 2019, doi: 10.3390/en12244624.
[15] E. H. Herraprastanti and W. A. Saputro, "Simulation of opening angle of Archimedes wind turbine design based on the Fibonacci series," *International Journal of Engineering, Science and Information Technology*, vol. 2, no. 1, pp. 50–57, Nov. 2021, doi: 10.52088/ijesty.v2i1.192.
[16] M. A. A. Nawar, H. S. A. Hameed, A. Ramadan, Y. A. Attai, and M. H. Mohamed, "Experimental and numerical investigations of the blade design effect on Archimedes spiral wind turbine performance," *Energy*, vol. 223, p. 120051, May 2021, doi: 10.1016/j.energy.2021.120051.
[17] A. M. Labib, A. F. A. Gawad, and M. M. Nasseif, "Effect of blade angle on aerodynamic performance of Archimedes spiral wind turbine," *Journal of Advanced Research in Fluid Mechanics and Thermal Sciences*, vol. 78, no. 1, pp. 122–136, Dec. 2020, doi: 10.37934/arfmts.78.1.122136.
[18] K. Kim, H. Ji, Y. Kim, Q. Lu, J. Baek, and R. Mieremet, "Experimental and numerical study of the aerodynamic characteristics of an Archimedes spiral wind turbine blade," *Energies*, vol. 7, no. 12, pp. 7893–7914, Nov. 2014, doi: 10.3390/en7127893.
[19] H. Hamid and R. M. Abd El Maksoud, "A comparative examination of the aerodynamic performance of various seashell-shaped wind turbines," *Heliyon*, vol. 9, no. 6, p. e17036, Jun. 2023, doi: 10.1016/j.heliyon.2023.e17036.
[20] K. A. Adeyeye, N. Ijumba, and J. Colton, "The effect of the number of blades on the efficiency of a wind turbine," *IOP Conference Series: Earth and Environmental Science*, vol. 801, no. 1, p. 012020, Jun. 2021, doi: 10.1088/1755-1315/801/1/012020.
[21] R. Roohi and M. Akbari, "Performance enhancement of parabolic dish collector receiver using phase change material: a CFD simulation," *Journal of Renewable Energy and Environment*, vol. 11, no. 1, pp. 38–45, 2024, doi: 10.30501/jree.2023.349281.1393.
[22] A. E. Faisal *et al.*, "Investigating the techniques used for improving the aerodynamic performance of Archimedes spiral wind turbines: a comprehensive review and future work avenues," *Results in Engineering*, vol. 25, p. 103992, Mar. 2025, doi: 10.1016/j.rineng.2025.103992.
[23] A. M. Kamal, M. A. A. Nawar, Y. A. Attai, and M. H. Mohamed, "Blade design effect on Archimedes spiral wind turbine performance: experimental and numerical evaluations," *Energy*, vol. 250, p. 123892, Jul. 2022, doi: 10.1016/j.energy.2022.123892.
[24] R. Supreeth, S. K. Maharana, and K. Bhaskar, "Whale-inspired tubercles for passively enhancing the performance of a wind turbine blade," *International Journal of Renewable Energy Research*, vol. 13, no. 1, pp. 489–503, 2023, doi: 10.20508/ijrer.v13i1.12713.g8707.
[25] P. I. Muiruri, O. S. Motsamai, and R. Ndeda, "A comparative study of RANS-based turbulence models for an upscale wind turbine blade," *SN Applied Sciences*, vol. 1, no. 3, 2019, doi: 10.1007/s42452-019-0254-5.
[26] A. G. Gonzalez-Rodriguez, J. M. Roldan-Fernandez, and L. M. Nieto-Nieto, "Unveiling inertia constants by exploring mass distribution in wind turbine blades and review of the drive train parameters," *Machines*, vol. 11, no. 9, pp. 1–22, 2023, doi: 10.3390/machines11090908.

BIOGRAPHIES OF AUTHORS

Rosadila Febritasari has been at Mechanical Engineering Department of Malang National Institute of Technology, Indonesia, since 2022. She currently focuses on design and manufacturer field. She can be contacted at email: rosadila@lecturer.itn.ac.id.

Muhammad Ibnul Abidin currently working as laboratory asistant in Compuer Laboratory at Mechanical Engineering Department of Malang National Institute of Technology, Indonesia, since 2022. He experts in design and manufacturing field. He can be contacted at email: ibnulabidin5678@gmail.com.